Supporting information

Modulation of Photocatalytic Properties through Counter-ion Substitution: Tuning the Bandgaps of Aromatic Sulfonium Octamolybdates for Efficient Photo-degradation of Rhodamine B

Mahender Singh and Chullikkattil P. Pradeep*

*School of Basic Science, Indian Institute of Technology Mandi, Mandi – 175005, Himachal Pradesh, India.

Fax: +91 1905 267 009; Tel: +91 1905 267 045; E-mail: pradeep@iitmandi.ac.in

Table of contents

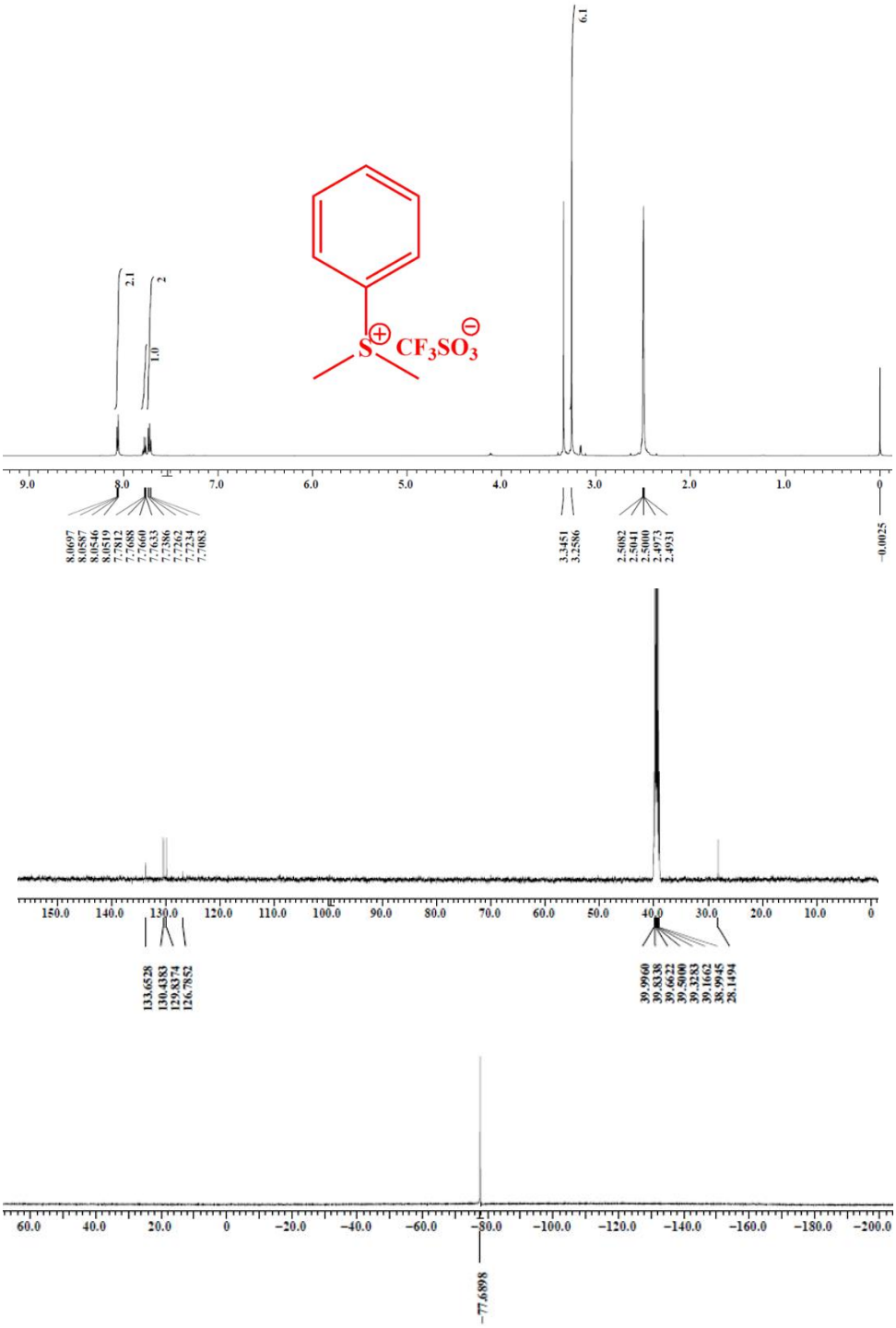

Fig. S1 ^{1}H, ^{13}C, and ^{19}F NMR spectra of DMPST in DMSO-d_6.

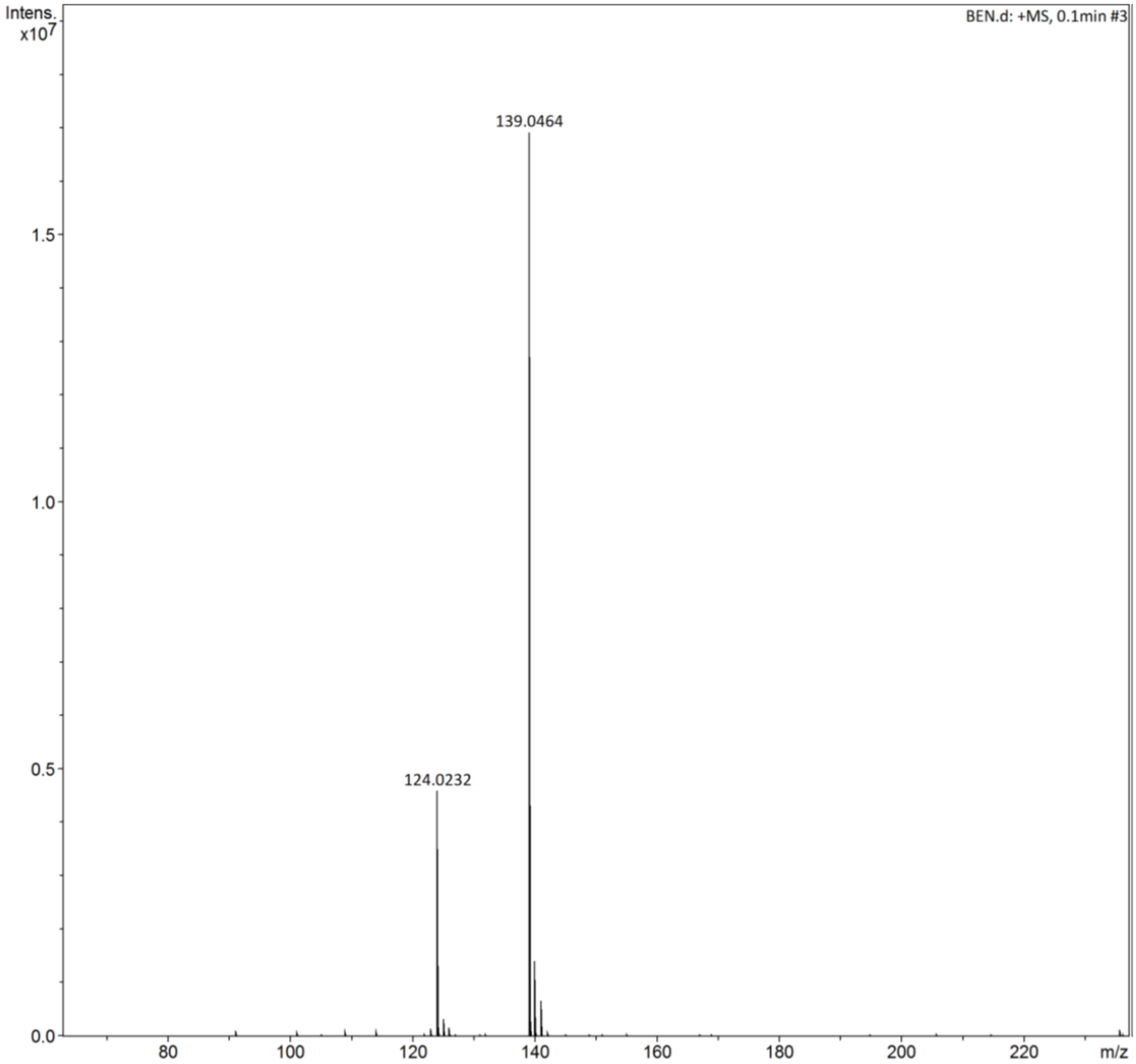

Fig. S2 Mass spectrum of DMPST.

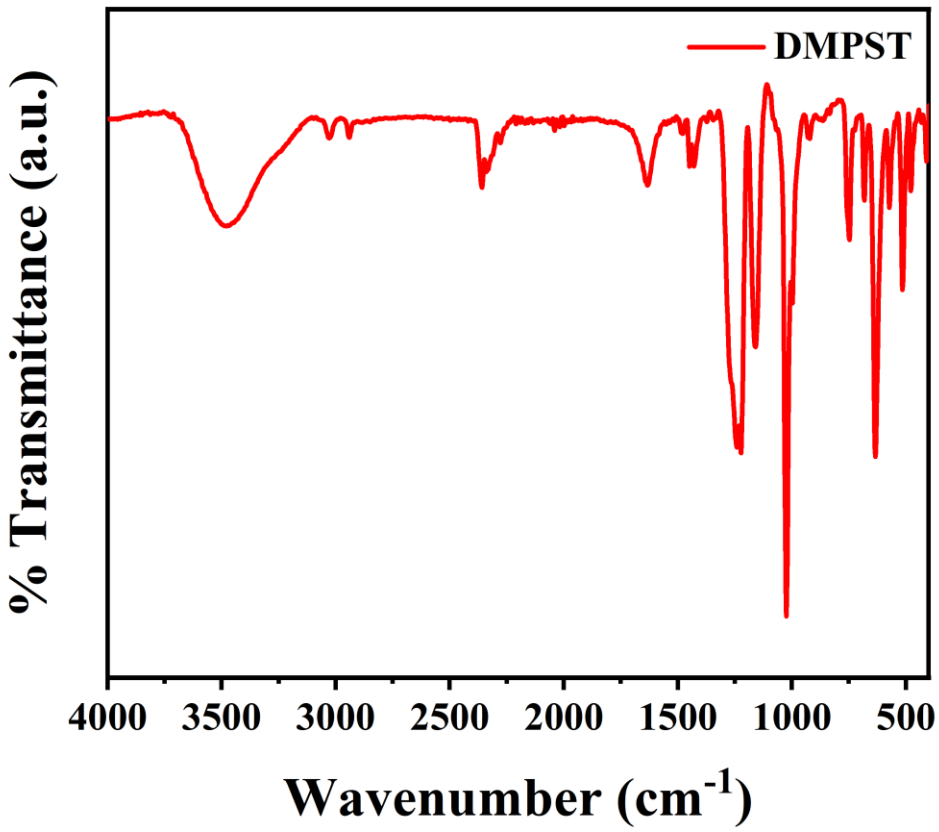

Fig. S3 FT-IR spectrum of DMPST.

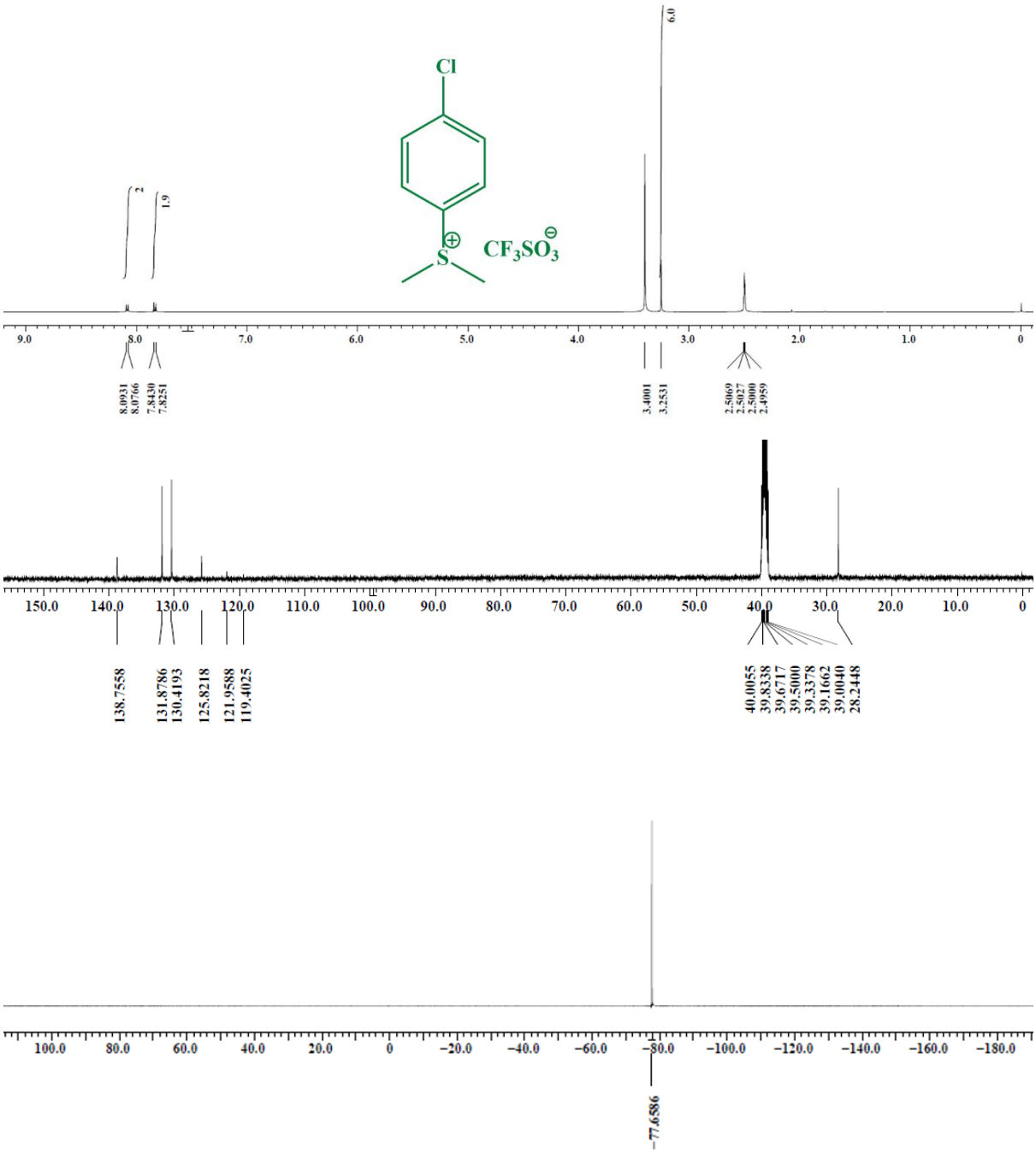

Fig. S4 ^{1}H, ^{13}C, and ^{19}F NMR spectra of CPDST in DMSO-d_6.

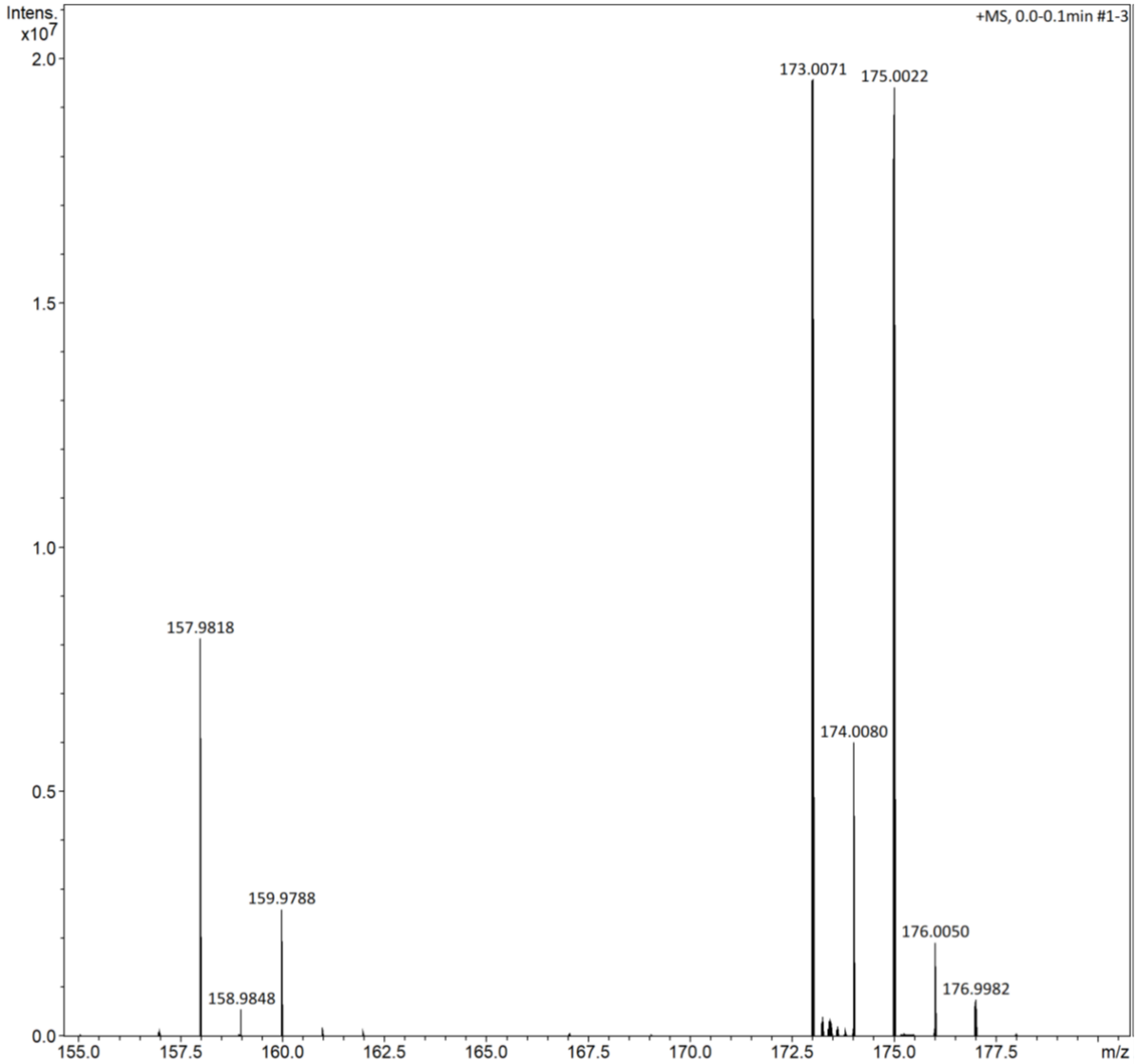

Fig. S5 Mass spectrum of CPDST.

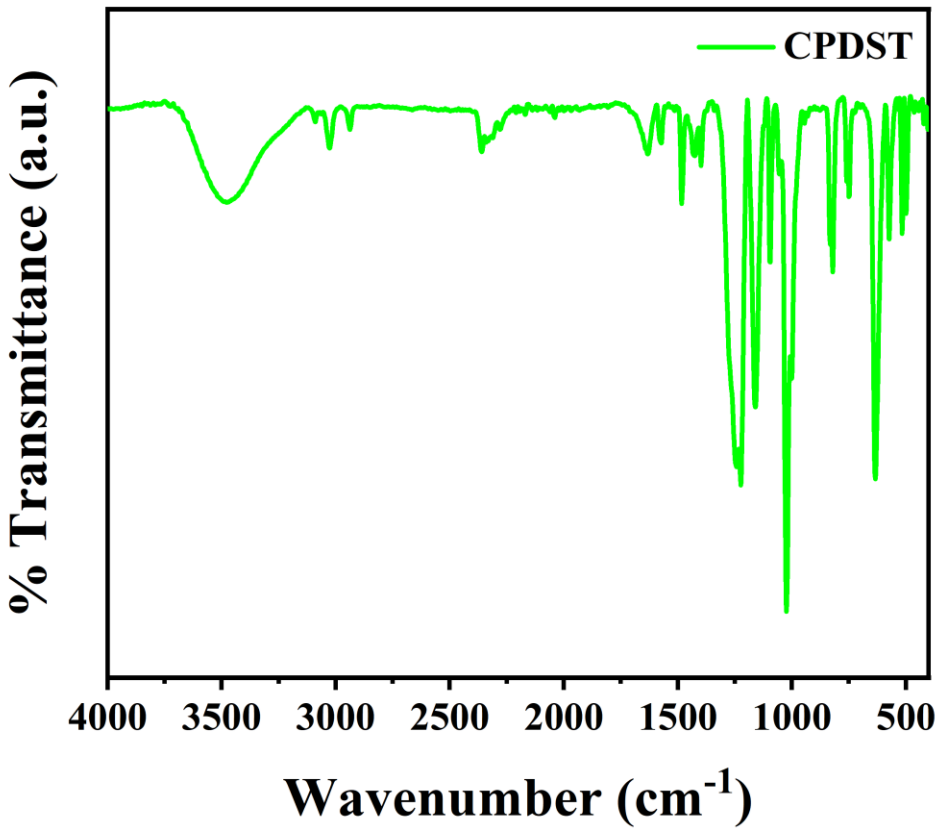

Fig. S6 FT-IR spectrum of CPDST.

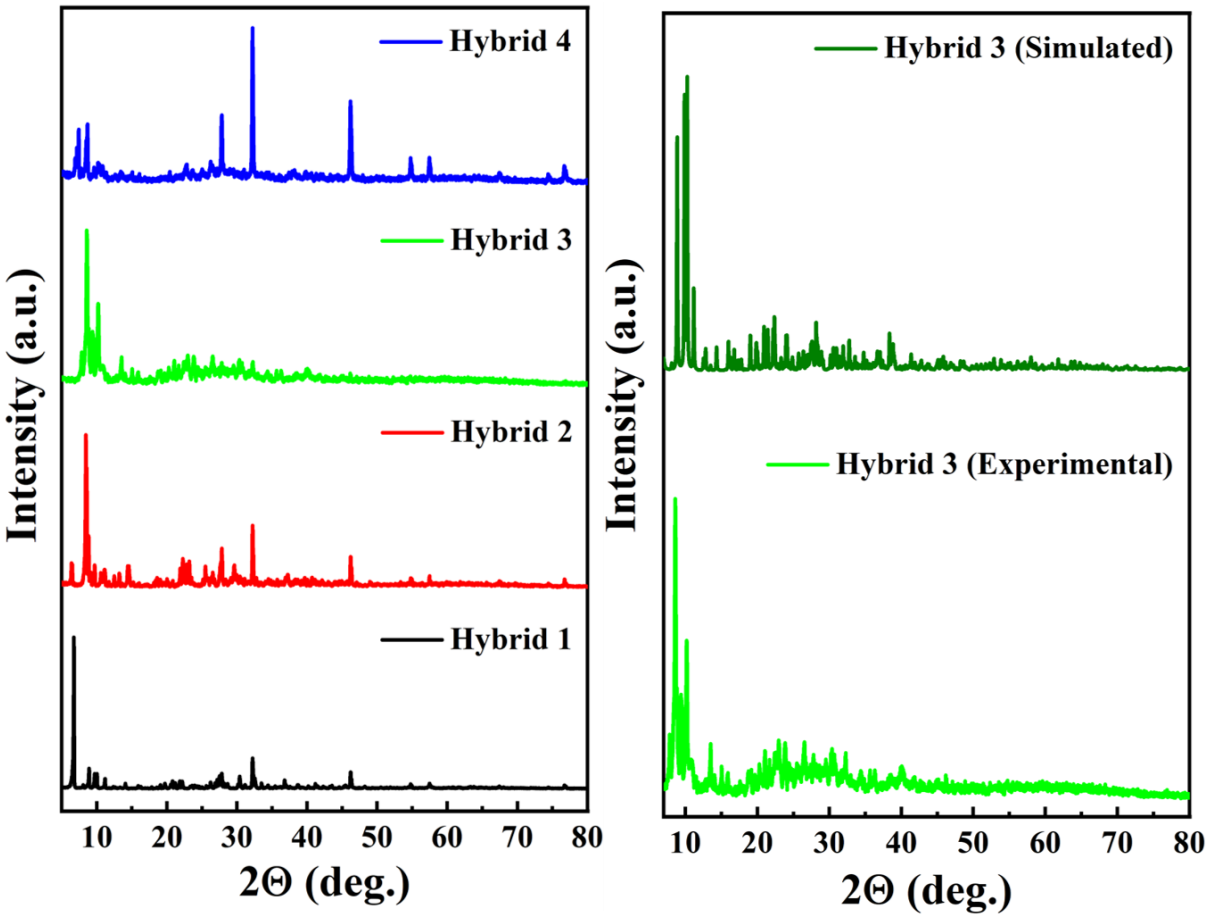

Fig. S7 The powder X-rays diffraction pattern of (a) hybrid **1-4** and (b) simulated and observed pattern of hybrid **3**.

Table S1. XPS atomic percentage analysis of different Mo oxidation state in hybrid **1-4**.

Sr. No.	**Mo**	**Hybrid 1**	**Hybrid 2**	**Hybrid 3**	**Hybrid 4**
1.	**$Mo^{6+}3d_{5/2}$(%)**	48.46	48.82	50.90	42.12
2.	**$Mo^{6+}3d_{3/2}$(%)**	34.15	33.83	34.70	33.91
3.	**$Mo^{5+}3d_{5/2}$(%)**	15.16	14.75	12.17	19.77
4.	**$Mo^{5+}3d_{3/2}$(%)**	2.24	2.61	2.23	4.20

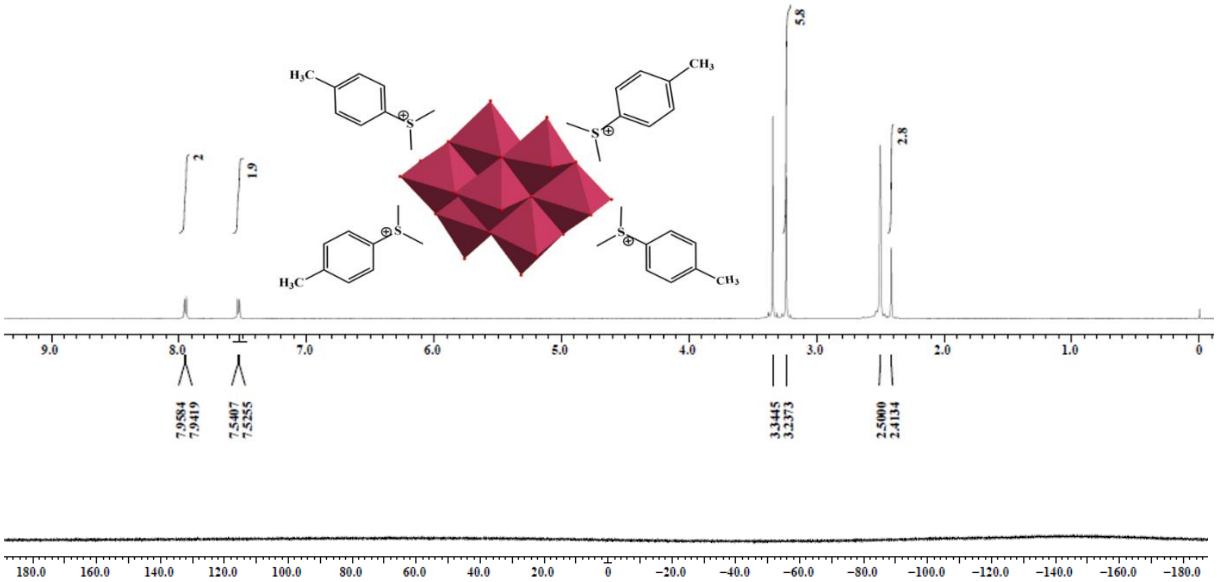

Fig. S8 ^{1}H, ^{19}F NMR spectra of hybrid **1** in DMSO-d_6.

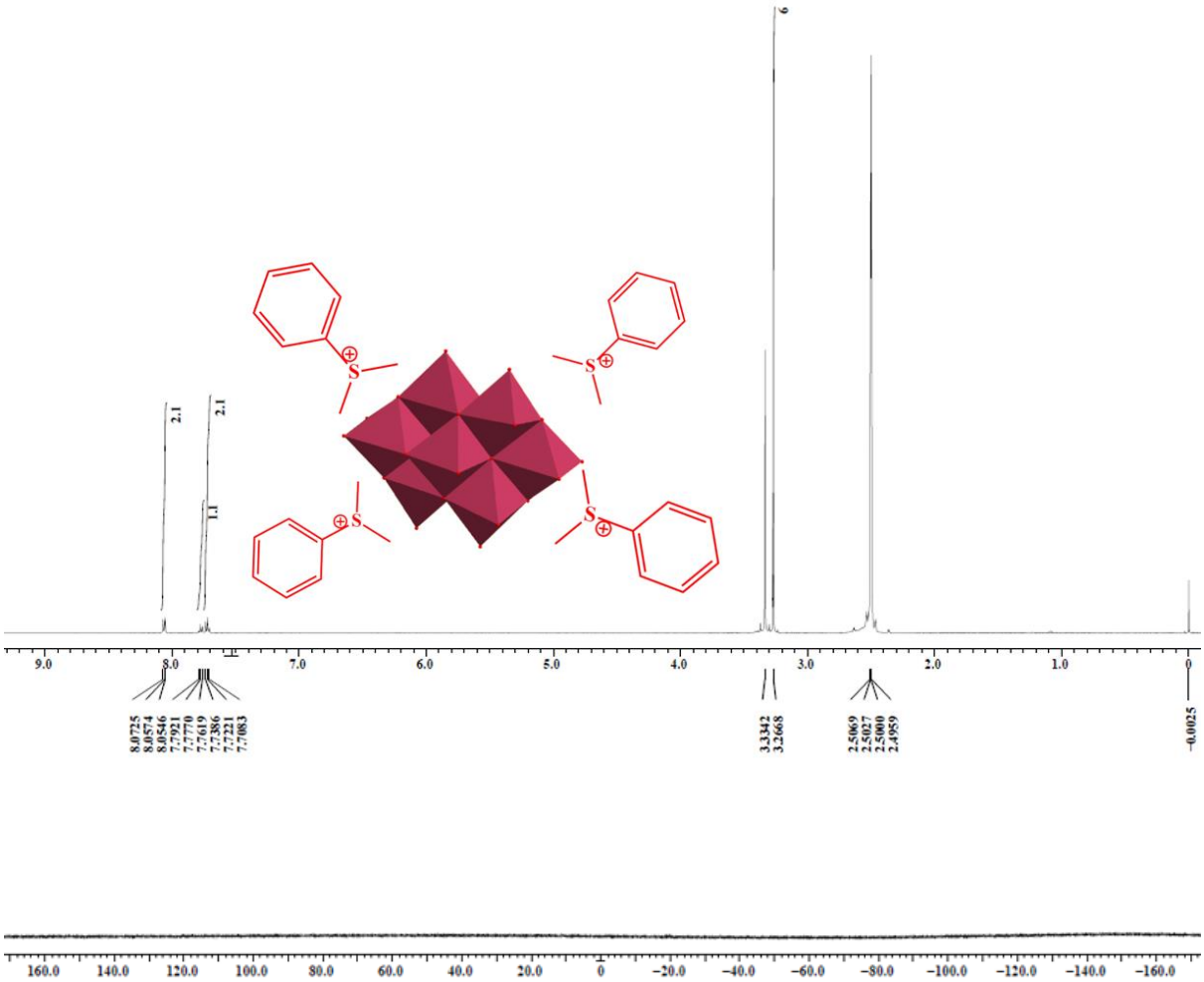

Fig. S9 ^{1}H, ^{19}F NMR spectra of hybrid **2** in DMSO-d_6.

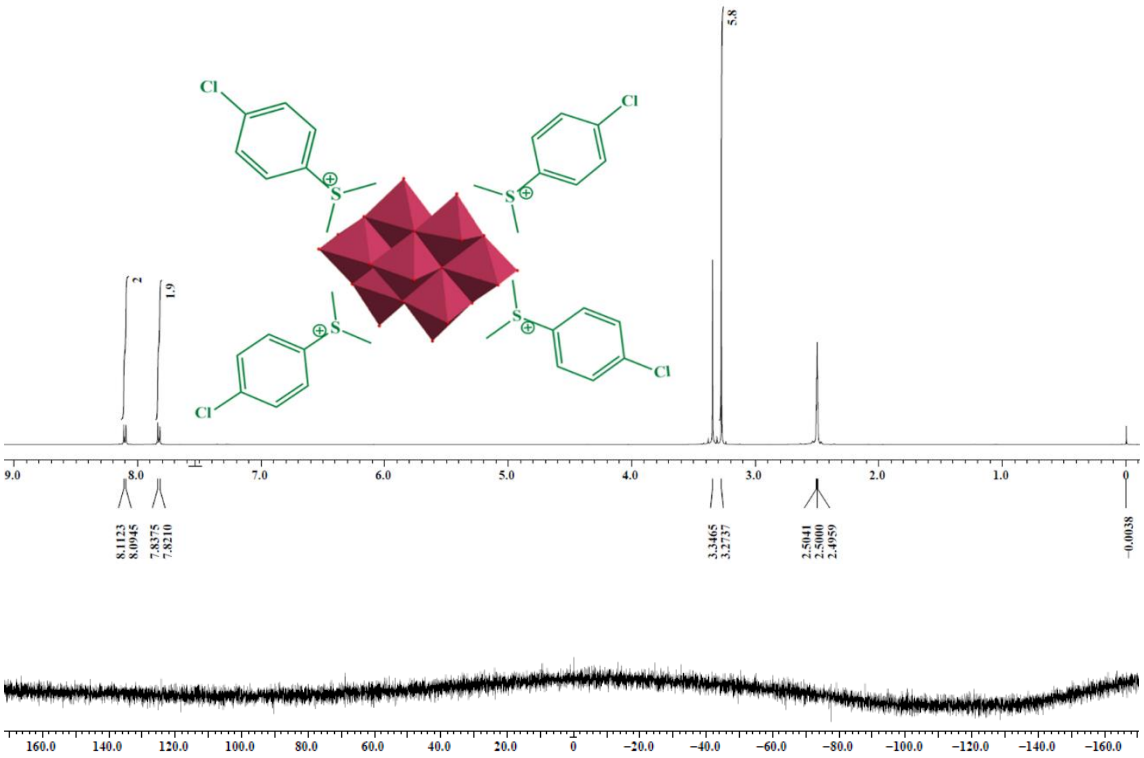

Fig. S10 ^{1}H, ^{19}F NMR spectra of hybrid **3** in DMSO-d_6.

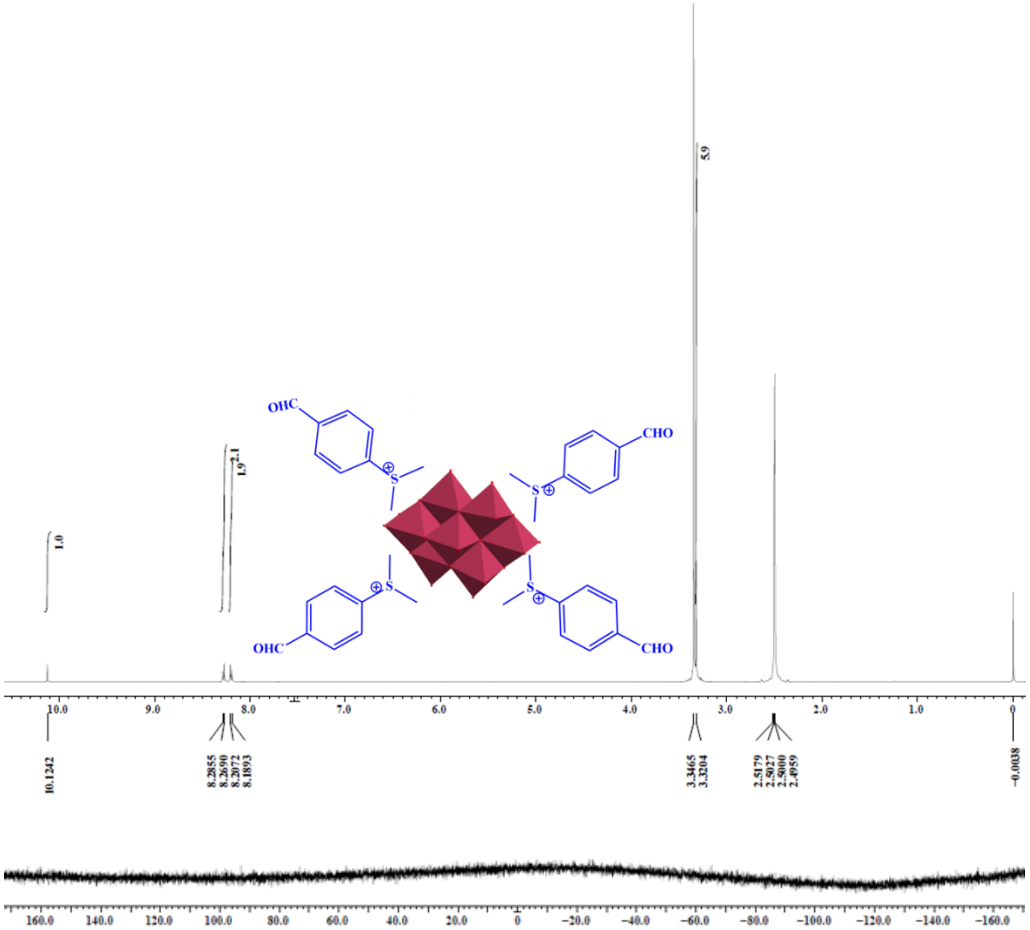

Fig. S11 ^{1}H, ^{19}F NMR spectra of hybrid **4** in DMSO-d

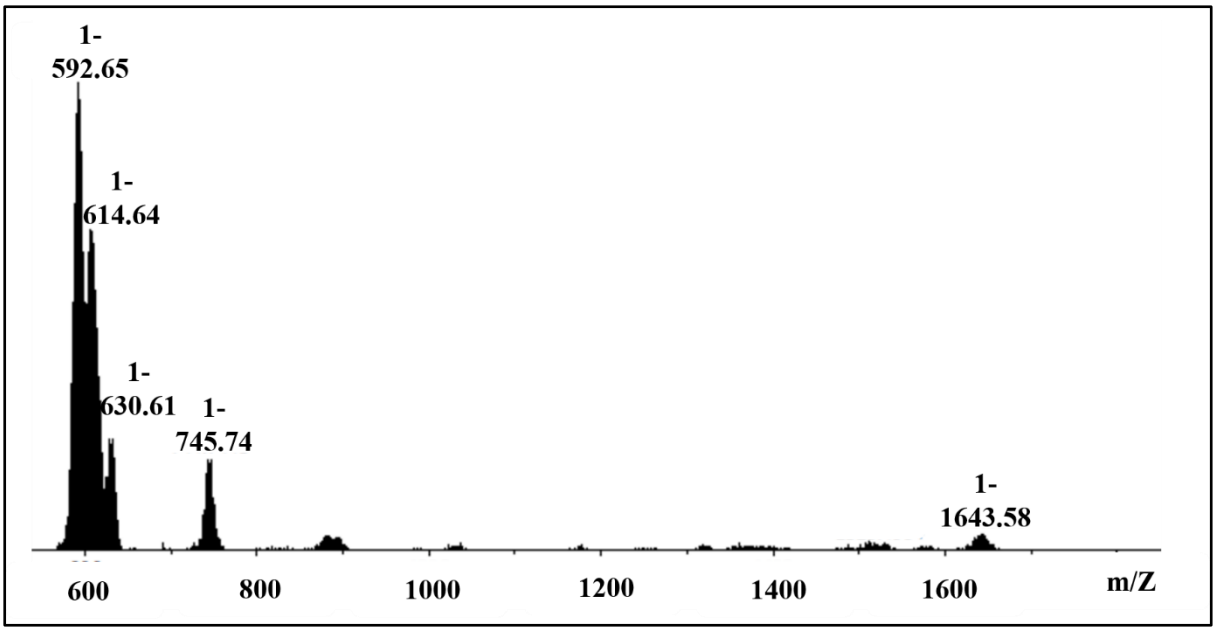

Fig. S12 ESI – MS (negative mode) spectra of hybrid **1** recorded in acetonitrile.

Table S2. Detailed assignment of mass spectral data for hybrid **1**.

Sr. No.	Ion (hybrid 1)	m/Z calculated	m/Z observed
1.	$(H)[Mo_4O_{13}]^{1-}$	592.76	592.65
2.	$(Na)[Mo_4O_{13}]^{1-}$	614.74	614.64
3.	$(K)[Mo_4O_{13}]^{1-}$	630.85	630.61
4.	$(DMTS)[Mo_4O_{13}]^{1-}$	745.02	745.74
5.	$(DMTS)_3[Mo_8O_{26}]^{1-}$	1643.30	1643.58

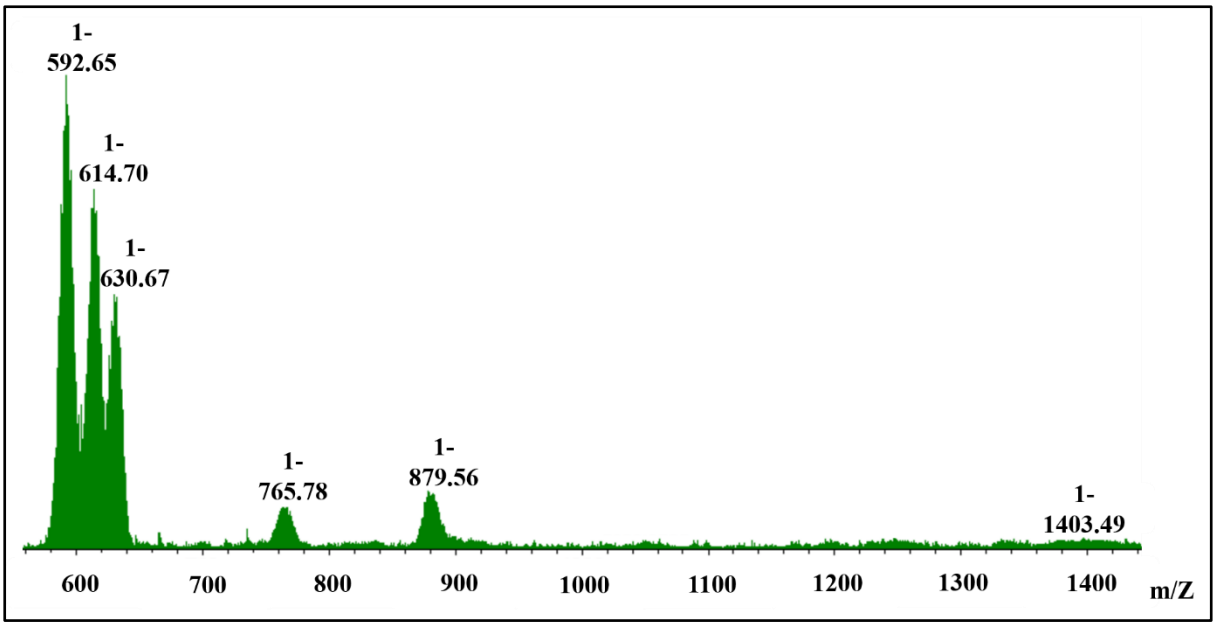

Fig. S13 ESI – MS (negative mode) spectra of hybrid **3** recorded in acetonitrile.

Table S3. Detailed assignment of mass spectral data for hybrid **3**.

Sr. No.	Ion (hybrid 3)	m/Z calculated	m/Z observed
1.	$(H)[Mo_4O_{13}]^{1-}$	592.76	592.65
2.	$(Na)[Mo_4O_{13}]^{1-}$	614.74	614.70
3.	$(K)[Mo_4O_{13}]^{1-}$	630.85	630.67
4.	$(CPDS)[Mo_4O_{13}]^{1-}$	765.43	765.78
5.	$(CPDS)(Na)[HMo_4O_{13}]^{1-}.5H_2O$	879.51	879.56
6.	$(CPDS)(Na_2)[Mo_8O_{26}]^{1-}$	1403.17	1403.49

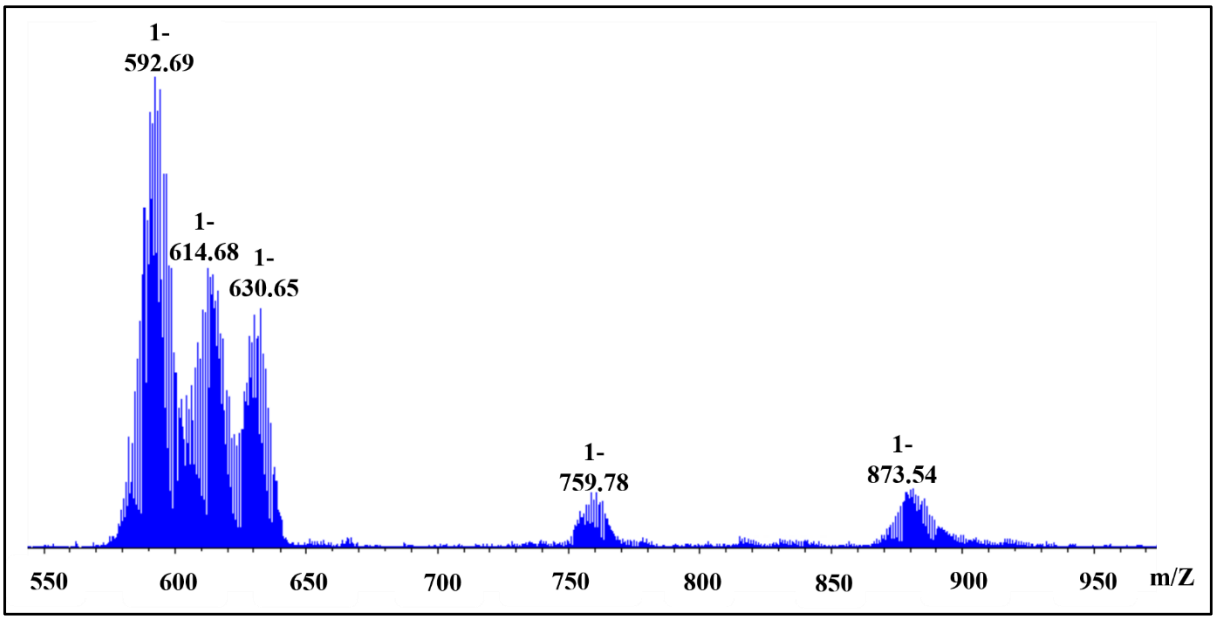

Fig. S14 ESI – MS (negative mode) spectra of hybrid **4** recorded in acetonitrile.

Table S4. Detailed assignment of mass spectral data for hybrid **4**.

Sr. No.	Ion (hybrid 4)	m/Z calculated	m/Z observed
1.	$(H)[Mo_4O_{13}]^{1-}$	592.76	592.69
2.	$(Na)[Mo_4O_{13}]^{1-}$	614.74	614.68
3.	$(K)[Mo_4O_{13}]^{1-}$	630.85	630.65
4.	$(FPDS)[Mo_4O_{13}]^{1-}$	759.00	759.78
5.	$(FPDS)(Na)[HMo_4O_{13}]^{1-}.5H_2O$	873.07	873.54

Table S5. Crystallographic data and structure refinement parameters of hybrid **3**·$2H_2O$.

Empirical formula	$C_{32}H_{44}Cl_4Mo_8O_{28}S_4$
Formula weight	1914.214
Temperature/K	150.01(11)
Crystal system	monoclinic
Space group	$P2_1/c$
a/Å	13.7572(4)
b/Å	19.9652(6)
c/Å	10.5884(3)
α/°	90.00
β/°	108.704(3)
γ/°	90.00
Volume/$Å^3$	2754.68(15)
Z	2
D_c (mg m^{-3})	2.308
μ/mm^{-1}	2.188
F(000)	1831.4
Crystal size/mm^3	0.248 × 0.179 × 0.122
Radiation	Mo Kα (λ = 0.71073)
2Θ range for data collection/°	3.74 to 56.74
Index ranges	$-18 \leq h \leq 12$, $-20 \leq k \leq 26$, $-9 \leq 1 \leq 13$
Reflections collected	9379
Independent reflections	5955 [R_{int} = 0.0370, R_{sigma} = 0.0691]
Data/restraints/parameters	5955/0/350
Goodness-of-fit on F^2	1.041
Final R indexes [I>=2σ (I)]	R_1 = 0.0367, wR_2 = 0.0705
Final R indexes (all data)	R_1 = 0.0566, wR_2 = 0.0894
Largest diff. peak and hole (e. $Å^{-3}$)	0.91/-1.06

Table S6. Properties of rhodamine B (RhB) dye.

Parameter	Value
Name of dye	Rhodamine B
Abbreviation	RhB
Color index number	45170
C. I. name	Basic Violet 10
Molecular formula	$C_{28}H_{31}N_2O_3Cl$
Molecular weight	479.02 g/mol
Type	Cationic
λ_{max}	553 nm
Chemical structure	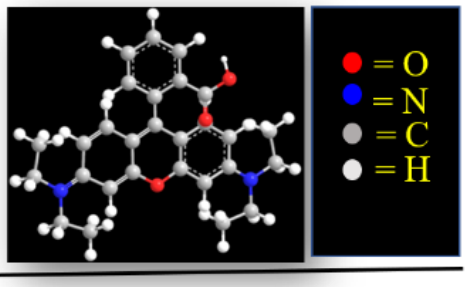

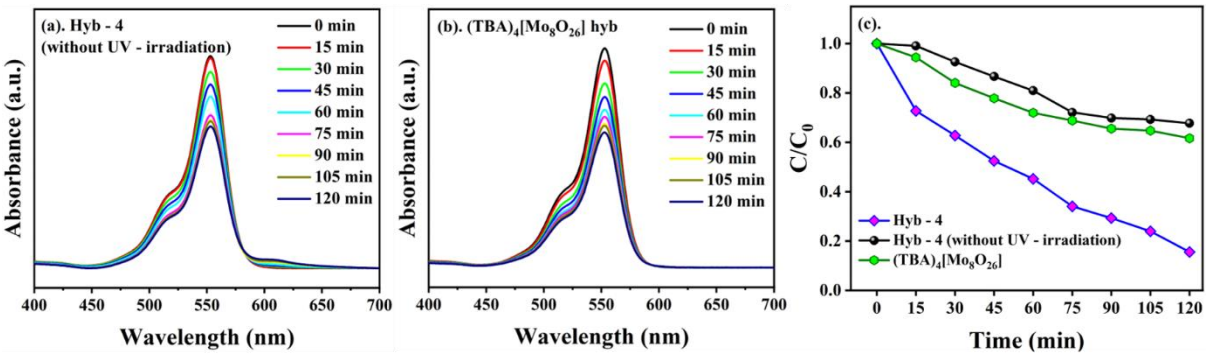

Fig. S15 The control experiment for RhB removal with (a) hybrid **4** without irradiation of UV – light, (b) with tetrabutylammonium octamolybdate hybrid $(TBA)_4[Mo_8O_{26}]$ in the presence of UV – light and (c) the comparison of amount of RhB concentration change with hybrid **4** with or without UV – light and with $(TBA)_4[Mo_8O_{26}]$ hybrid in the presence of UV - light .

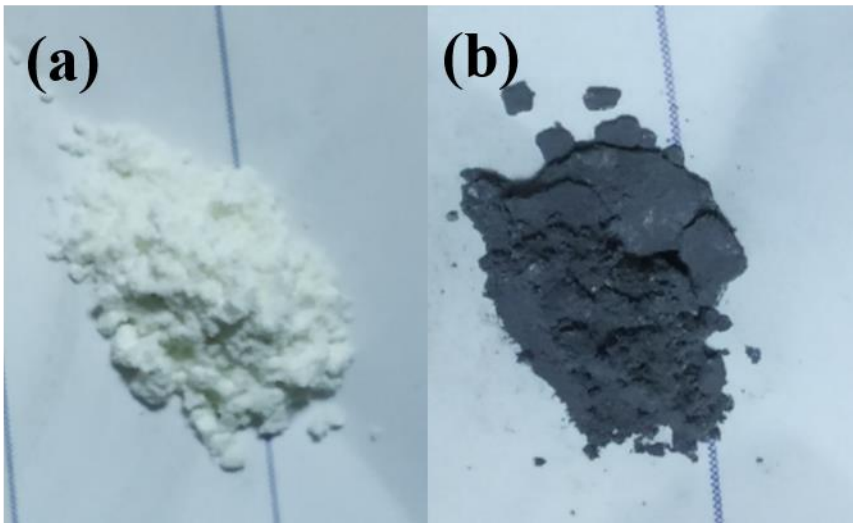

Fig. S16 The images of hybrid **4** sample powders (a) fresh sample and (b) after keeping for 2 h in DI water under UV – irradiation.

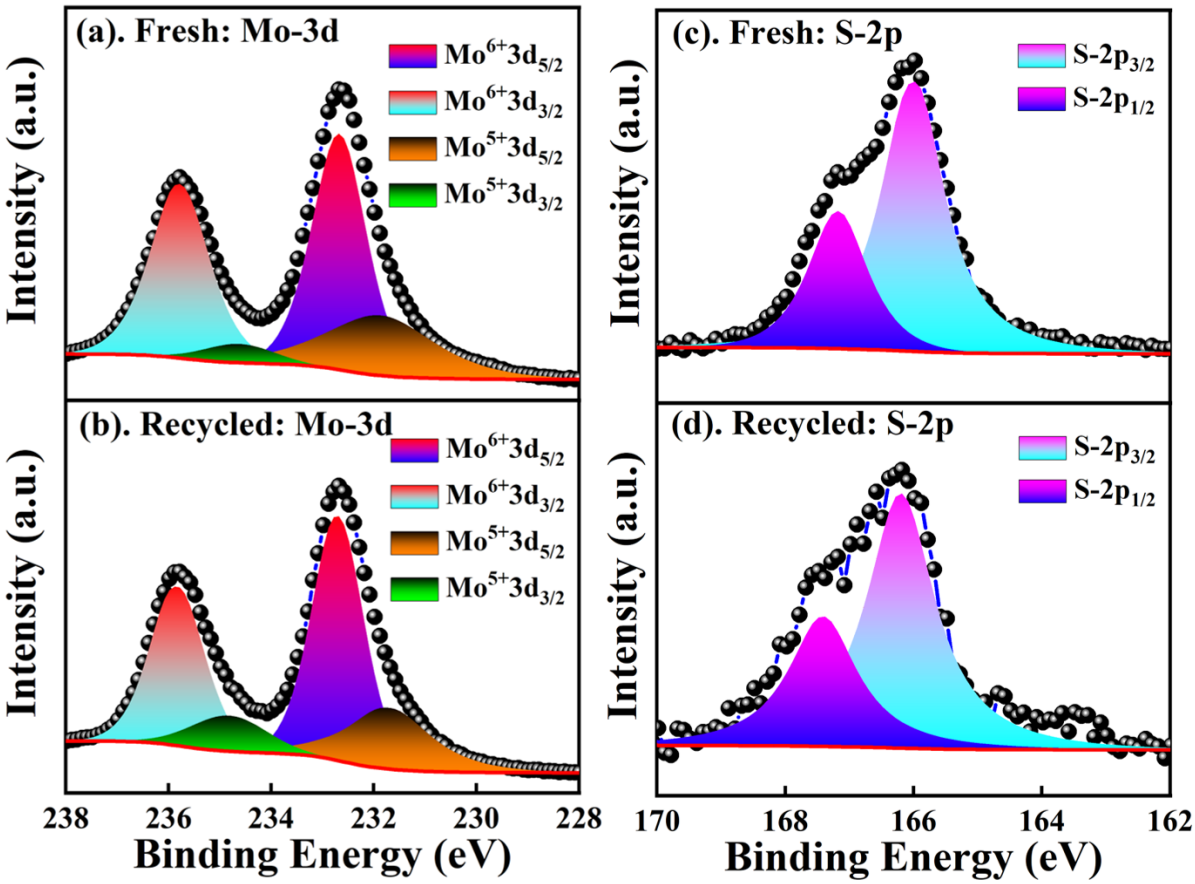

Fig. S17 The XPS spectra of hybrid **4** (a and c) fresh catalyst and (b-d) recycled catalyst showing deconvoluted Mo and S peaks.

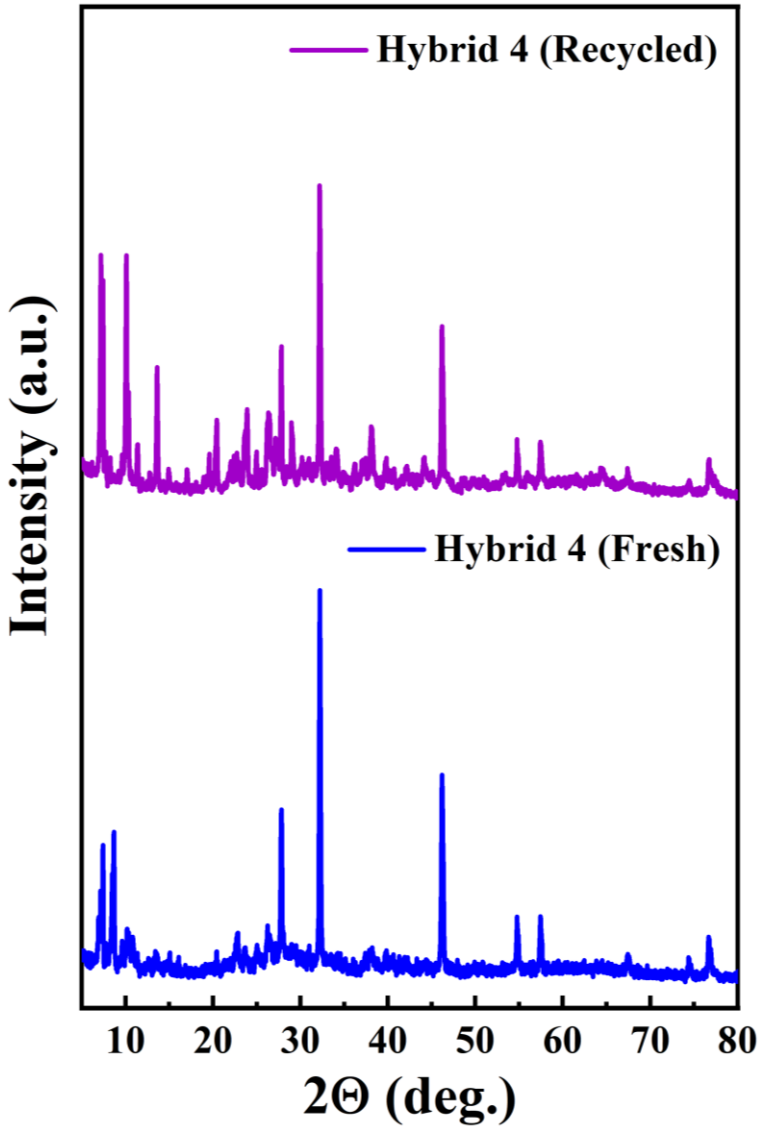

Fig. S18 The PXRD spectra of hybrid **4**, fresh and recycled catalyst.

Table S7. Comparison of the photocatalytic activity of hybrid **4** with several other octamolybdate base photocatalysts for RhB photodegradation.

Sr. No.	Photocatalyst	Radiation source	Time (min)	Total degradation (%)	Ref.
1.	$[Co(btrp)_2(H_2O)_2(\beta\text{-}Mo_8O_{26})_{0.5}]H_2O$	Simulate sunlight – Xe lamp irradiation (5000 LUX)	435	94.08	1
2.	$[Co(HL)_2(\beta\text{-}Mo_8O_{26})]$	UV-irradiation – Hg lamp (125 W)	180	Very low	2
3.	$[Cu_3(TPMA)_2(1,3\text{-}ttb)_2(\beta\text{-}Mo_8O_{26})]\cdot H_2O$	UV irradiation Hg lamp (100 W)	180	70	3
4.	$[Cu^{II}_4(btmc)(ctcm)_4(\beta\text{-}Mo_8O_{26})]\cdot[\beta\text{-}Mo_8O_{26}]\cdot H_2O$	UV irradiation	120	51.5	4
5.	$[Cu(4\text{-}Hdpyp)_2(\beta\text{-}Mo_8O_{26})(H_2O)_2]\cdot 4H_2O$	UV light irradiation – Hg lamp (125 W)	180	59.4	5
6.	$(FPDS)_4[Mo_8O_{26}]$ – Hybrid 4	UV irradiation – Hg lamp (8 W)	120	84.4	This work

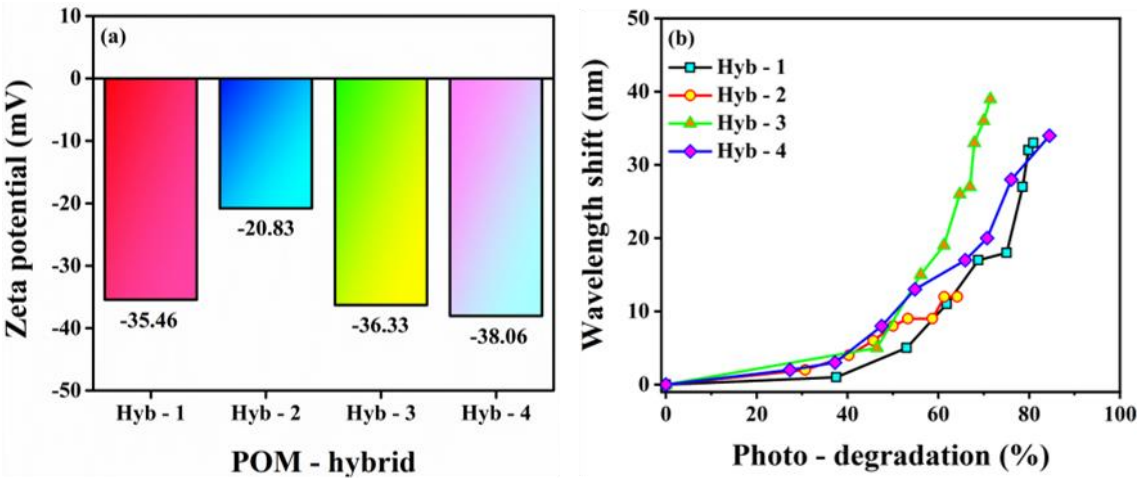

Fig. S19 (a) Zeta potential of different hybrids at 4.65 pH and (b) maximum absorption wavelength shift of RhB as a function of degradation percentage with different POM – hybrids.

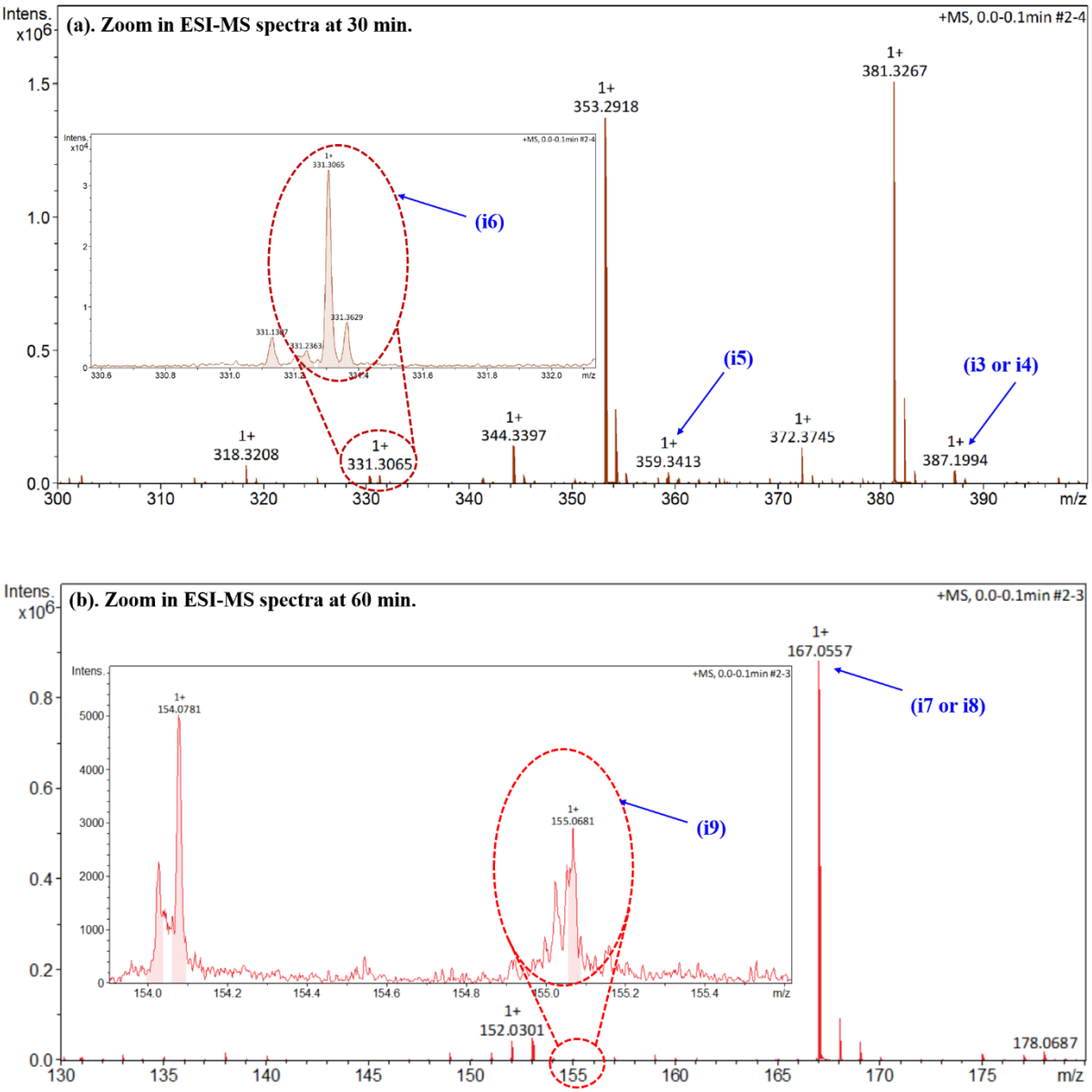

Fig. S20 Zoom in ESI – MS spectra (positive ion mode) of photodegraded RhB dye at (a) 30 min showing the presence of intermediate i3 or i4, i-5, i6 and (b) 60 min showing the presence of intermediate i7 or i8 and i9.

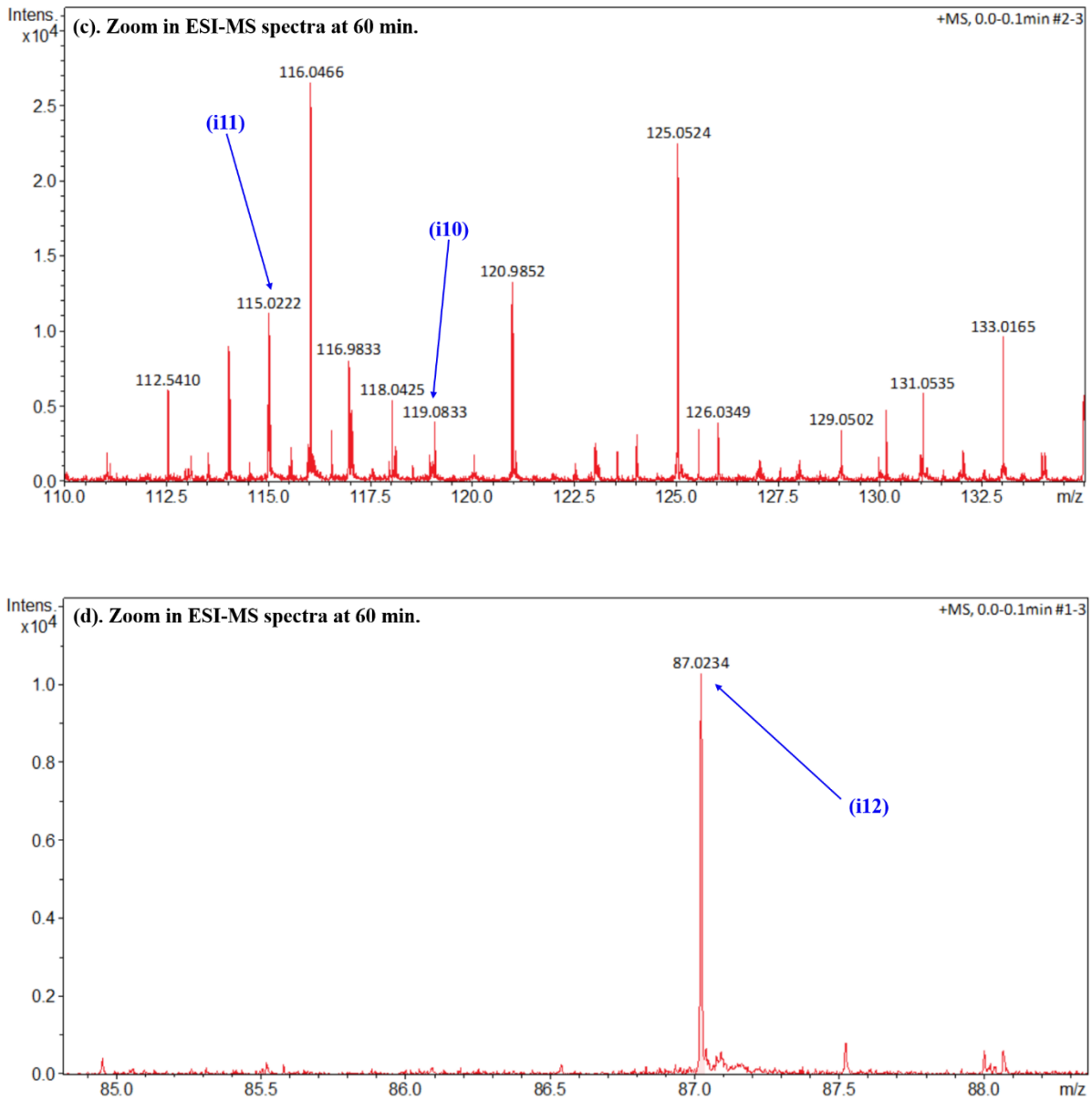

Fig. S21 Zoom in ESI – MS spectra (positive ion mode) of photodegraded RhB dye at 60 min showing the presence of intermediate (c) i10, i11 and (d) i12.

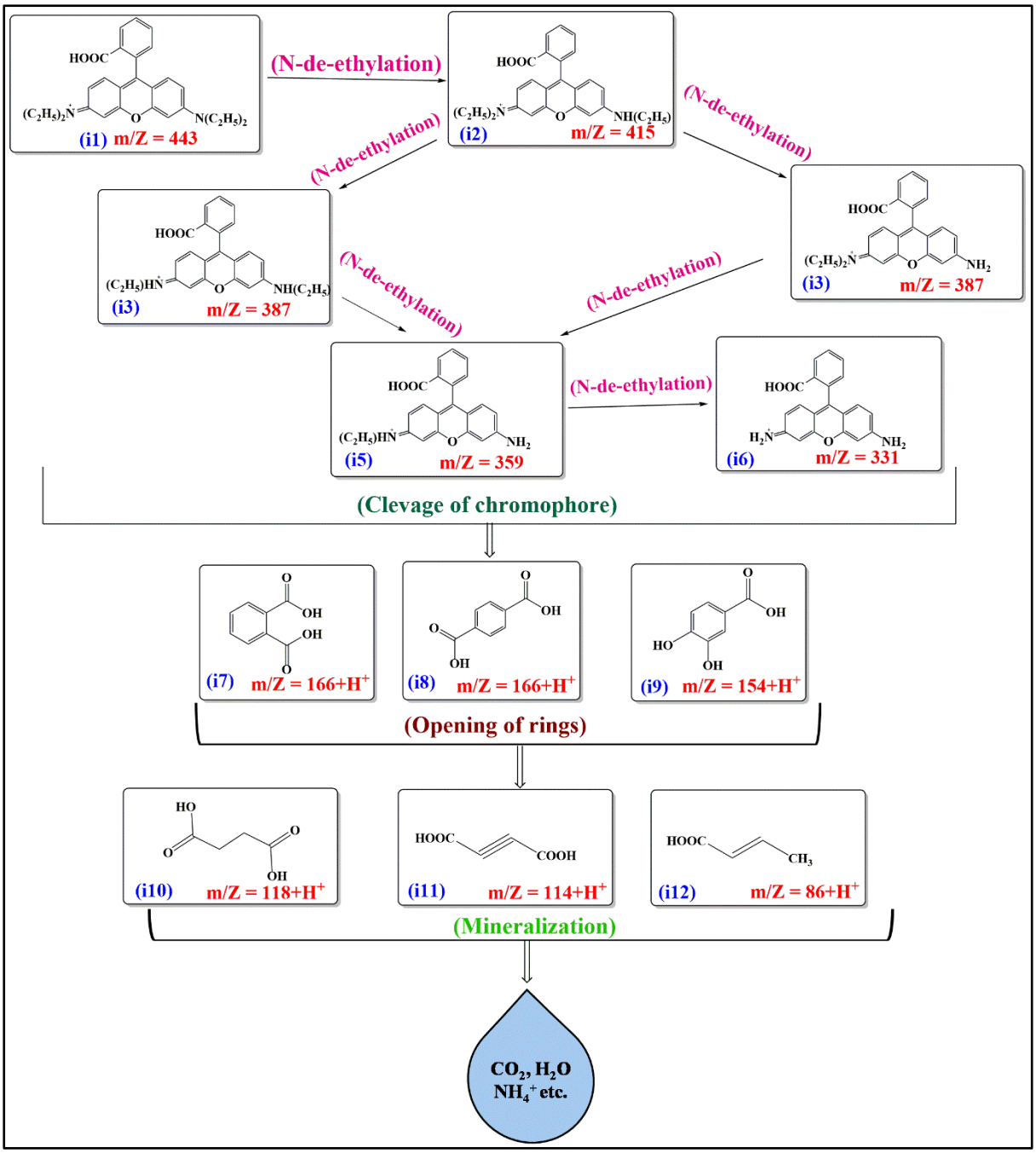

Scheme S1 Plausible pathways and fragments formed during RhB dye photodegradation using hybrid **4**.

Table S8. Various intermediates involved in RhB dye photodegradation their chemical composition, expected and observed m/Z value.

Sr. No.	Intermediate	Chemical formula	Expected mass (m/Z)	Observed mass (m/Z)
1.	(i1)	$[C_{28}H_{31}N_2O_3]^+$	443.233	443.281
2.	(i2)	$[C_{26}H_{27}ON_2O_3]^+$	415.202	415.237
3.	(i3) or (i4)	$[C_{24}H_{23}N_2O_3]^+$	387.170	387.199
4.	(i5)	$[C_{22}H_{19}N_2O_3]^+$	359.139	359.341
5.	(i6)	$[C_{20}H_{15}N_2O_3]^+$	331.108	331.306
6.	(i7 or i8)	$[C_8H_6O_4H]^+$	167.027	167.055
7.	(i9)	$[C_7H_6O_4H]^+$	155.027	155.068
8.	(i10)	$[C_4H_6O_4H]^+$	119.100	119.083
9.	(i11)	$[C_4H_2O_4H]^+$	115.060	115.022
10.	(i12)	$[C_4H_6O_2H]^+$	87.100	87.023

References

1. J. Chi, M. Fan, Z. Su, X. Li, J. Sun, C. Zhou and X. Hu, Octamolybdate-based hybrid constructed by flexible bis-triazole ligands: synthesis, photocatalytic and electrochemical properties, *New J. Chem.*, 2020, **44**, 13524-13528.
2. L. Li, X. Wang, N. Xu, Z. Chang, G. Liu, H. Lin and X. Wang, Four octamolybdate complexes constructed from a quinoline–imidazole–monoamide ligand: structures and electrochemical, photocatalytic and magnetic properties, *CrystEngComm.*, 2020, **22**, 8322-8329.
3. H. Guo, C. Gong, X. Zeng, H. Xu, Q. Zeng, J. Zhang, Z. Zhong and J. Xie, Isopolymolybdate-based inorganic–organic hybrid compounds constructed by multidentate N-donor ligands: syntheses, structures and properties, *Dalton Trans.*, 2019, **48**, 5541-5550.
4. C. Wang, J. Ying, H.-c. Mou, A.-x. Tian and X.-l. Wang, Multi-functional photoelectric sensors based on a series of isopolymolybdate-based compounds for detecting different ions, *Inorg. Chem. Front.*, 2020, **7**, 3882-3894.
5. X. Wang, J. Sun, H. Lin, Z. Chang, X. Wang and G. Liu, A series of Anderson-type polyoxometalate-based metal–organic complexes: Their pH-dependent electrochemical behaviour, and as electrocatalysts and photocatalysts, *Dalton Trans.*, 2016, **45**, 12465-12478.